Isabel N. Figueiredo
CMUC, Department of Mathematics, University of Coimbra, 3001-454 Coimbra, Portugal
E-mail address: isabelf@mat.uc.pt

Carlos Leal
CMUC, Department of Mathematics, University of Coimbra, 3001-454 Coimbra, Portugal
E-mail address: carlosl@mat.uc.pt

Giuseppe Romanazzi
CMUC, Department of Mathematics, University of Coimbra, 3001-454 Coimbra, Portugal
E-mail address: roman@mat.uc.pt

Bjorn Engquist
Department of Mathematics, University of Texas at Austin, Austin, TX 78712, USA
E-mail address: engquist@ices.utexas.edu

Pedro N. Figueiredo
Faculty of Medicine, University of Coimbra, and Department of Gastroenterology, University Hospital of Coimbra, Portugal
E-mail address: pedro.n.figueiredo@clix.pt

Pré-Publicações do Departamento de Matemática
Universidade de Coimbra
Preprint Number 10–44

A CONVECTION-DIFFUSION-SHAPE MODEL FOR ABERRANT COLONIC CRYPT MORPHOGENESIS

ISABEL N. FIGUEIREDO, CARLOS LEAL, GIUSEPPE ROMANAZZI, BJORN ENGQUIST AND PEDRO N. FIGUEIREDO

Abstract: It is generally accepted that colorectal cancer is initiated in the small pits, called crypts, that line the colon. Normal crypts exhibit a regular pit pattern, similar in two-dimensions to a U-shape, but aberrant crypts display different patterns, and in some cases show bifurcation. According to several medical articles, there is an interest in correlating pit patterns and the cellular kinetics, namely of proliferative and apoptotic cells, in colonic crypts. This paper proposes and implements a hybrid convection-diffusion-shape model for simulating and predicting what has been validated medically, with respect to some aberrant colonic crypt morphogenesis. The model demonstrates crypt fission, in which a single crypt starts dividing into two crypts, when there is an increase of proliferative cells. The overall model couples the cell movement and proliferation equations with the crypt geometry. It relies on classical continuum transport/mass conservation laws and the changes in the crypt shape are driven by the pressure exerted by the cells on the crypt wall. This pressure is related to the cell velocity by a Darcy-type law. Numerical simulations are conducted and comparisons with the medical results are shown.

Keywords: convection-diffusion equation, Darcy law, backward Euler method, finite elements, colonic crypts.

AMS Subject Classification (2000): 76R99, 35J15, 35R37, 65M06, 65M50, 65M60.

1. Introduction and motivation

Colorectal carcinoma (CRC) occurs as a consequence of several genetic mutations in normal colonic mucosa, determining phenotypic modifications with biological and morphologic consequences [12]. Those modifications lead to dysfunction of the cellular process and cause loss of homeostasis in colonic crypts.

In this context it is relevant correlating pit patterns and cellular kinetics in colonic crypts. This is precisely the primary goal of this paper. We introduce here a hybrid convection-diffusion-shape model for a single colonic

Received November 9, 2010.
This work is part of the research project UTAustin/MAT/0009/2008 of the UT Austin | Portugal Program (http://www.utaustinportugal.org/).

crypt. It simulates and predicts what has been validated medically (see [21, 38]), with respect to some aberrant colonic crypt morphogenesis. The model demonstrates crypt fission, in which a single crypt starts dividing into two crypts, when there is an increase of proliferative cells.

The overall model couples, in a two-dimensional setting, a convection-diffusion system, describing the cell movement and proliferation process inside the single crypt (based on classical continuum transport/mass conservation laws) with the crypt geometry.

For setting up the convection-diffusion system, we can assemble (in a simplest way, but without loss of generality) the different populations of cells, that reside inside the colonic crypt, into two large classes: proliferative and apoptotic cells, and consider that the sum of their densities is equal to one. This means that these two populations of cells are understood in a broad sense. The class of proliferative cells include stem, transit and/or semi-differentiated cells and the class of apoptotic cells include, as well, fully differentiated cells (see for instance [19] for a detailed description of the different cell sets). We also suppose the convective velocities of both proliferative and apoptotic cell densities are the same and furthermore this velocity obeys to a Darcy-type law (supposing that the cells flow trough the crypt, like fluid through a porous medium see [15, 35]). This means the convective velocity is related to an unknown pressure. This is also in good agreement with [24, 8, 42] , where it is assumed that the essential mechanism, responsible for the cell flux in the crypt, is the mitotic activity which causes pressure-driven passive movement. In addition, we can solve the convection-diffusion system only for the proliferative cell density and the results for the apoptotic cell density are subsequently inferred, because the sum of the densities is equal to one.

On the whole, the convection-diffusion system is a coupling of a parabolic type equation, whose unknown is the proliferative cell density, with an elliptic equation, whose unknown is the pressure (related to the convective velocity of the proliferative cells by Darcy's law mentioned above). The definitions for parameters involved in the convection-diffusion system (*i.e.*, rates of birth and death, and the diffusion for the proliferative cell density), as well as, the boundary and initial conditions are also explained in the paper and rely on some qualitative information reported in the literature. In particular, we suppose the rates of birth and death, are functions of the crypt height, which means they depend on the cell position. This is in good agreement with

[32] A. Quarteroni, L. Formaggia, and A. Veneziani (eds). *Complex systems in Biomedicine*. Springer-Verlag Italia, Milano, 2006.
[33] B. Ribba, T. Colin, and S. Schnell. A multiscale mathematical model of cancer, and its use in analyzing irradiation therapies. *Theoretical Biology and Medical Modelling*, (3:7), 2006.
[34] L. Roncucci, A. Medline, and W. R. Bruce. Classification of aberrant crypt foci and microadenomas in human colon. *Cancer Epidemiology, Biomarkers & Prevention*, 1:57–60, 1991.
[35] T. Roose, S. Jonathan Chapman, and P. K. Maini. Mathematical models of avascular tumor growth. *SIAM Review*, 49(2):179–208, 2007.
[36] J. A. Sherratt and M. A. Chaplain. A new mathematical model for avascular tumour growth. *Journal of Mathematical Biology*, 43:291–312, 2001.
[37] I-M. Shih et al. Top-down morphogenesis of colorectal tumors. *Proceedings of the National Academy of Sciences of the United States*, 98(5):2640–2645, 2001.
[38] S. Tamura, Y. Furuya, T. Tadokoro, Y. Higashidani, Y. Yokoyama, K. Araki, and S. Onishi. Pit pattern and three-dimensional configuration of isolated crypts from the patients with colorectal neoplasm. *Journal of Gastroenterology*, 37(10):798–806, 2002.
[39] R. W. Taylor et al. Mitochondrial DNA mutations in human colonic crypt stem cells. *The Journal of Clinical Investigation*, 112(9):1351–1360, 2003.
[40] The Mathworks, Inc. *http://www.matlab.com.*
[41] I. P. M. Tomlinson and W. F. Bodmer. Failure of programmed cell death and differentiation as causes of tumors: some simple mathematical models. *Proceedings of the National Academy of Sciences of the United States*, 92(9):11130–11134, 1995.
[42] I. M. M. van Leeuwen, H. M. Byrne, O. E. Jensen, and J. R. King. Crypt dynamics and colorectal cancer: advances in mathematical modelling. *Cell Proliferation*, 39:157–181, 2006.
[43] I. M. M. van Leeuwen, C. M. Edwards, M. Ilyas, and H. M. Byrne. Towards a multiscale model of colorectal cancer. *World Journal of Gastroenterology*, 13(9):1399–1407, 2007.
[44] I.M.M. van Leeuwen, H.M. Byrne, M.D. Johnston, C.M. Edwards, S.J. Chapman, W.F. Bodmer, and P.K. Maini. Modelling multiscale aspects of colorectal cancer. In *CP971, International Conference on Mathematical Biology -ICMB07*, pages 3–7, 2008. American Institute of Physics Conference Proceedings.
[45] A. C. Walter. *A Comparison of Continuum and Cell-based Models of Colorectal Cancer*. PhD thesis, University of Nottingham, March 2009.
[46] J. P. Ward and J. R. King. Mathematical modelling of avascular-tumor growth. *IMA Journal of Mathematics Applied in Medicine and Biology*, 14:39–69, 1997.
[47] D. Wodarz. Effect of stem cell turnover rates on protection against cancer and aging. *Journal of Theoretical Biology*, 245:449–458, 2007.

[13] J. Galle, M. Loeffler, and D. Drasdo. Modeling the effect of deregulated proliferation and apoptosis on the growth dynamics of epithelial cell populations in vitro. *Biophysical Journal*, 88:62–75, 2005.
[14] L. C Greaves et al. Mitochondrial DNA mutations are established in human colonic stem cells, and mutated clones expand by crypt fission. *Proceedings of the National Academy of Sciences of the United States*, 103(3):714–719, 2006.
[15] H. P. Greenspan. On the growth and stability of cell cultures and solid tumors. *Journal of Theoretical Biology*, 56(2):229–242, 1976.
[16] P. R. Harper and S. K. Jones. Mathematical models for the early detection and treatment of colorectal cancer. *Health Care Management Science*, 8:101–109, 2005.
[17] C.S. Hogea, B.T. Murray, and J. A. Sethian. Simulating complex tumor dynamics from avascular to vascular growth using a general level-set method. *Journal of Mathematical Biology*, 53(1):86–134, 2006.
[18] D. Hurlstone et al. Rectal aberrant crypt foci identified using high-magnification-chromoscopic colonoscopy: biomarkers for flat and depressed neoplasia. *American Journal of Gastroenterology*, pages 1283–1289, 2005.
[19] M. D. Johnston, C.M. Edwards, W. F. Bodmer, P. K. Maini, and S. J. Chapman. Mathematical modeling of cell population dynamics in the colonic crypt and in colorectal cancer. *Proceedings of the National Academy of Sciences of the United States*, 104(10):4008–4013, 2007.
[20] Y. Kato. Mixed-type boundary conditions for second order elliptic differential equations. *J. Math. Soc. Japan*, 26:405–432, 1974.
[21] Y. Kutarani, S. Tamura, Y. Furuya, and S. Onishi. Morphogenesis of a colorectal neoplasm with a type iiis pit pattern inferred from isolated crypts. *Journal of Gastroenterology*, 43:597–602, 2008.
[22] P. Macklin and J.S. Lowengrub. A new ghost cell/level set method for moving boundary problems: application to tumor growth. *Journal of Scientific Computing*, 35(2-3):266–299, 2008.
[23] N. V. Mantzaris, S. Webb, and H. G. Othmer. Mathematical modeling of tumor-induced angiogenesis. *Journal of Mathematical Biology*, 49:111–187, 2004.
[24] F. A. Meineke, C. S. Potten, and M. Loeffler. Cell migration and organization in the intestinal crypt using a lattice-free model. *Cell Proliferation*, 34(4):253–266, 2001.
[25] F. Michor, Y. Iwasa, C. Lengauer, and M. A. Nowak. Dynamics of colorectal cancer. *Seminars in Cancer Biology*, 15:484–494, 2005.
[26] J. D. Murray. *Mathematical biology: II. Spatial Models and Biomedical Applications*, volume 18 of *Interdisciplinary Applied Mathematics: Mathematical Biology*. Springer-Verlag, Berlin, 2004.
[27] C. V. Pao. *Nonlinear parabolic and elliptic equations*. Plenum Press, New York, 1992.
[28] U. Paulus, M. Loeffler, J. Zeidler, G. Owen, and C.S. Potten. The differentiation and lineage development of goblet cells in the murine small intestinal crypt: experimental and modelling studies. *Journal of Cell Science*, 106:473–484, 1993.
[29] P. F. Pinsky. A multi-stage model of adenoma development. *Journal of Theoretical Biology*, 207:129–143, 2000.
[30] S. L. Preston, W.-M. Wong, A. O.-O. Chan, R. Poulsom, R. Jeffery, R.A. Goodlad, N. Mandir, G. Elia, M. Novelli, W.F. Bodmer, I.P. Tomlinson, and N.A. Wright. Bottom-up histogenesis of colorectal adenomas: Origin in the monocryptal adenoma and initial expansion by crypt fission. *Cancer Research*, 63:3819–3825, 2003.
[31] L. Preziosi and A. Farina. On Darcy's law for growing porous media. *International Journal of Non-Linear Mechanics*, 37:485–491, 2002.

experimental evidence, as reported in [44], where it is suggested "parameters controlling cellular process may depend on biochemical and bio-mechanical signals and, thus, on cell position". Then, the changes in the crypt geometry are essentially ruled by the pressure exerted by the cells on the crypt wall. In addition, some bio-mechanical assumptions, establishing a relation between the movement of the different boundaries of the crypt, are also imposed.

In the paper we basically focus on two problems. In the first, called the normal case, we derive values for the parameters, boundary and initial conditions aiming at preserving the normal geometry of the colonic crypt, as well as, at keeping a stabilized distribution of the density of proliferative cells and pressure values, with time, and along the crypt axis. In the second, called the abnormal case, we first increase the rate of birth of proliferative cells at the bottom of the crypt. Secondly, using the information on the pressure value, obtained in the normal case, we change one boundary condition for the pressure. This is done in an appropriate way and based on bio-mechanical reasoning. The model then leads to an aberrant crypt shape exhibiting fission.

We emphasize, that the model proposed in this paper, does not provide any justification for the increase of the rate of birth of proliferative cells. The main goal is just to infer what is the deformation produced by this increase in the crypt geometry.

In the literature, a reasonable collection of articles concerning the mathematical modelling of cell populations in individual colonic crypts can be found, as well as works dealing with the mathematical modelling of colorectal cancer and, more generally, of tumor growth. We refer, in particular, to [3, 6, 8, 7, 13, 19, 28, 41, 42] for models concerning dynamics of cell populations, to [5, 9, 16, 25, 33, 42, 43, 47] for papers reporting models related to colorectal cancer, to [1, 2, 15, 23, 26, 29, 31, 32, 36] for the mathematical modelling of tumor growth, and also [17, 22], where the level set technique is used to model the tumor's boundary in time, and finally to [11, 14, 18, 30, 34, 37, 39] for some medical papers related to aberrant crypt foci and colorectal cancer. To the best of our knowledge, there are no mathematical models in the literature reporting the connection between cellular kinetics and colonic crypt patterns, as done here in this paper. The results presented here follows our previous work [10], where we used a convection-diffusion type equation coupled with a level set equation, for tracking the time evolution of an epithelial cell set, inside a colonic crypt, until it reaches

the top of the crypt. However, in [10], the modifications induced on geometry of the crypt, by the cells, were not considered.

After this introduction, this paper is organized in the following way. In section 2 preliminaries of the mathematical model are defined together with some explanations, based on known medical and biological information, which support the model definition. Afterwards, sections 3 and 4 describe the normal and abnormal cases, respectively, and include the corresponding model discretizations, and numerical algorithms for their approximate solutions. The simulations and comparisons with the medical results are shown in sections 3.2.1 and 4.2.1. Finally in the last section there are some comments and outlook work.

2. Mathematical models - preliminaries

The epithelium of the colon is perforated by millions of small crypts, which play a crucial role in colon physiology. In effect, the colon epithelium undergoes a complete renewal, by means of a programmed mechanism driven by the cellular kinetics inside the crypts [19, 42]. Each crypt has a cylindrical tube shape, that is closed at the bottom and with a round opening in the top, directed at the lumen's colon. Different types of cells fill the crypt. These are aligned along the crypt wall: stems cells are believed to reside in the bottom of the crypt, transit cells along the middle part of the crypt axis and differentiated cells at the top of the crypt. In normal human colonic crypts, the cells renew completely each 3-6 days, through an harmonious and ordered procedure which includes the proliferation of cells, their migration along the crypt wall towards the top and their apoptosis, as they reach the orifice of the crypt and the cell cycle is finished.

For defining the mathematical model proposed in this paper, we use a two-dimensional (2D) version of a colonic crypt. A vertical cut (*i.e.* along the crypt axis) of a normal crypt shows a thin and long U-shape (see the medical sub-figure 1 (a) right). In sub-figure 1 (b) it is depicted a schematic U-shape of this vertical cut: (O, X, Y) represents a Cartesian system, with origin O, Ω_c stands for the 2D-geometry of the crypt, and the rectangle Ω subset of $\mathbb{R}2$ represents the portion of the colon where the crypt is located. The boundaries of Ω_c are also represented: Γ_1 is the upper boundary (directed to the lumen of the colon), Γ_2 and Γ_3 are respectively, the outer and inner boundaries. It is worth mentioning that for humans, the average dimensions of a normal crypt are: $73\mu m$, the height $433\mu m$ for the height (where $1\mu m = 10^{-6}m$)

boundary conditions, with respect to N, replaced by $\gamma\frac{\partial N}{\partial n} + \eta N = 0$, is in $C^\infty(\Omega_c \times]0, T])$. Moreover if the initial condition $N0 \in C^\infty(\Omega_c)$ is positive, then $N \in C^\infty(\Omega_c \times]0, T])$ is also positive.

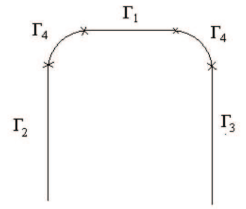

FIGURE 5. Modified crypt boundary

References

[1] T. Alarcón, H. M. Byrne, and P. K. Maini. Towards whole-organ modelling of tumour growth. *Progress in Biophysics & Molecular Biology*, 85:451–472, 2004.
[2] R. P. Araujo and L. S. McElwain. A history of the study of solid tumour growth: the contribution of mathematical modelling. *Bulletin of Mathematical Biology*, 66(1039–1091), 2004.
[3] N. J. Armstrong, K. J. Painter, and J. A. Sherratt. A continuum approach to modelling cell–cell adhesion. *Journal of Theoretical Biology*, 243:98–113, 2006.
[4] R. E. Baker, E. A. Gaffney, and P. K. Maini. Partial differential equations for self-organization in cellular and developmental biology. *Nonlinearity*, 21(11):R251–R290, 2008.
[5] M. Bienz and H. Clevers. Linking colorectal cancer to Wnt signaling. *Cell*, 103:311–320, 2000.
[6] B. M. Boman, J. Z. Fields, O. Bonham-Carter, and O. A. Runquist. Computer modeling implicates stem cell overproduction in colon cancer initiation. *Cancer Research*, 61:8408–8411, 2001.
[7] A. d'Onofrio and I. P. M. Tomlinson. A nonlinear mathematical model of cell turnover, differentiation and tumorigenesis in the intestinal crypt. *Journal of Theoretical Biology*, 244:367–374, 2007.
[8] D. Drasdo and M. Loeffer. Individual-based models to growth and folding in one-layered tissues: intestinal crypts and early development. *Nonlinear Analysis*, 47:245–256, 2001.
[9] C. M. Edwards and S.J. Chapman. Biomechanical modelling of colorectal crypt budding and fission. *Bulletin of Mathematical Biology*, 69(6):1927–1942, 2007.
[10] I.N. Figueiredo, C. Leal, T. Leonori, G. Romanazzi, P.N. Figueiredo, and M.M. Donato. A coupled convection-diffusion level set model for tracking epithelial cells in colonic crypts. *Procedia Computer Science*, 1(1):955–963, 2010.
[11] P. Figueiredo and M. Donato. Cyclooxygenase-2 is overexpressed in aberrant crypt foci of smokers. *European Journal of Gastroenterology & Hepatology*, 22(10):1271, 2010.
[12] P. Figueiredo, M. Donato, M. Urbano, H. Goulão, H. Gouveia, C. Sofia, M. Leitão, and Diniz Freitas. Aberrant crypt foci: endoscopic assessment and cell kinetics characterization. *International Journal of Colorectal Disease*, 24(4):441–450, 2009.

and dead cells, residing inside a single crypt, with the shape of the crypt. It was set up based on the cellular mechanism, that occurs in colonic crypts, and which is reported in several biological and medical articles.

On the whole, the numerical simulations, produced with the proposed model, reveal a good agreement with medical images exhibiting normal and bifurcated colonic crypts, obtained with scanning electron microscopy (see [21]). In addition, the simulations also demonstrate that a single crypt changes its geometric pattern and starts bifurcating at the bottom, where an abnormal increase of proliferative cells is taking place.

However, there is a need for further research, mainly with respect to the parameters involved in the model. In effect, these parameters rule the outcome of the numerical simulations. Yet, there is lack of information about their values, and they are very unlikely (or impossible) to be determined or tested experimentally. In the future we intend to address this issue. We will try to figure out these parameter values, based on the available qualitative information, and using again a mathematical approach.

Appendix. Given $N(.,t)$ it is well known that the elliptic problem,

$$\begin{cases} -\Delta p = \nabla \cdot (D\nabla N(.,t)) + \alpha N(.,t) & \text{in} \quad \Omega_c, \\ p = 1 & \text{in} \quad \Gamma_1, \\ \frac{\partial p}{\partial n} = 0 & \text{in} \quad (\Gamma_2 \cup \Gamma_3), \end{cases} \tag{24}$$

has a solution and that its regularity depends on the regularity of $N(.,t)$. However, the mixed Dirichlet-Neumann boundary conditions lead to a lack of regularity of p in the corner points connecting Dirichlet and Neumann boundary conditions. For ensuring the regularity of p in all the domain, the crypt Ω_c can be redefined in a natural way, by removing the corners (see Figure 5, which displays one upper branch of the redefined 2D-crypt) and modifying the boundary conditions in (24) (see [20] for a similar procedure). This means, $\partial\Omega_c = \Gamma_1 \cup \Gamma_2 \cup \Gamma_3 \cup \Gamma_4$, and the solution of (24) becomes $p = 1 + \bar{p}$, where $\bar{p}$ is the solution of

$$\begin{cases} -\Delta p = \nabla \cdot (D\nabla N(.,t)) + \alpha N(.,t) & \text{in} \quad \Omega_c, \\ \gamma \dfrac{\partial p}{\partial n} + \eta p = 0 & \text{in} \quad \partial\Omega_c, \end{cases} \tag{25}$$

where γ and η are non negative enough smooth functions in $\partial\Omega_c$, such that $\gamma + \eta = 1$, $\eta = 1$ in Γ_1, $\eta = 0$ in Γ_2. Assuming, furthermore that $N(.,t) \in C^\infty(\Omega_c)$, then the solution of (25) is in $C^\infty(\Omega_c)$. As a consequence, we can guarantee (see for instance [27]), that for a fixed $p = 1 + \bar{p}$ (with $\bar{p}$ solution of (25)) the solution N of the parabolic-type equation with the two

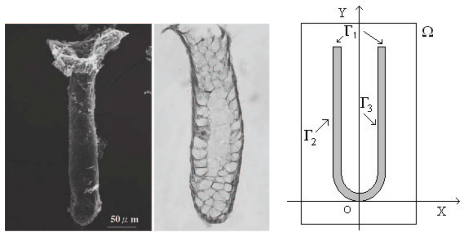

(a) (b)

FIGURE 1. (a) Medical images (from [38], with permission of Springer): scanning electron microscope image of an isolated crypt (in the left) and corresponding normal histopathologically vertical cut section (in the right). (b) Schematic vertical cut of a normal colonic crypt Ω_c and corresponding three boundaries.

and the thickness of the inner epithelium is about the size of a single cell. The relation between the height and the diameter has been preserved in the definition of the $2D$-domain Ω_c (see section 3.2.1).

We use a transport/mass conservation model to describe the dynamics of different types of cells inside a colonic the crypt. Furthermore, we adopt a two phase model, where only proliferative and apoptotic cells are considered. The transit cells are then included in the proliferative cell group. In addition, we suppose the proliferative cells move in a convective and diffusive manner (the apoptotic cells do not have random motion). Thus denoting by N_1 and N_2, the densities of proliferative and apoptotic cells, respectively, these equations are

$$\begin{cases} \frac{\partial N_1}{\partial t} + \nabla \cdot (v_1 N_1) = \nabla \cdot (D\nabla N_1) + \alpha N_1 - \beta N_1 & \text{in } \Omega_c \times (0,T), \\ \frac{\partial N_2}{\partial t} + \nabla \cdot (v_2 N_2) = \beta N_1 & \text{in } \Omega_c \times (0,T), \end{cases} \tag{1}$$

where D is the diffusion coefficient (it can be a scalar or a function), v_1 and v_2 are the convective velocities of N_1 and N_2, respectively, α and β the rates of birth and death of the proliferative cells N_1. It is usual to assume $v_1 = v_2 = v$ (see [35]). We also suppose the overall density of cells verify $N_1 + N_2 = 1$. So, summing the two equations in (1), we get

$$\nabla \cdot v = \nabla \cdot (D\nabla N_1) + \alpha N_1. \tag{2}$$

Furthermore, we assume that the interior of the colonic crypt is "fluid-like" and the cells flow through the fixed extracellular matrix like flow through a porous media, obeying to Darcy's law [33, 15, 46]. Therefore, the convective

velocity is defined by

$$v = -\nabla p, \tag{3}$$

where p is an (unknown) internal pressure. Consequently, by introducing (3) in (2) and gathering the result with (1) yields the system

$$\begin{cases} \frac{\partial N_1}{\partial t} - \nabla \cdot (\nabla p N_1) = \nabla \cdot (D \nabla N_1) + \alpha N_1 - \beta N_1 & \text{in } \Omega_c \times (0,T), \\ \frac{\partial N_2}{\partial t} + \nabla \cdot (\nabla p N_2) = \beta N_1 & \text{in } \Omega_c \times (0,T), \\ -\Delta p = \nabla \cdot (D \nabla N_1) + \alpha N_1 & \text{in } \Omega_c \times (0,T). \end{cases} \tag{4}$$

Remark 2.1. *We remark that instead of the condition $N_1 + N_2 = 1$, we could use the volume conservation relation $V_1 N_1 + V_2 N_2 = 1$, where V_1 and V_2 are, respectively, the averages volumes of the live and dead cells* [46]. *Then, the third equation in* (4) *would be*

$$-\Delta p = \nabla \cdot \big(D \nabla (V_1 N_1)\big) + (\alpha V_1 - \beta V_1 + \beta V_2) N_1$$

which is essentially of the same type.

Since the constraint $N_1 + N_2 = 1$ is not explicitly enforced in (4), we solve this system only for N_1, hereafter denoted by N, and infer the solution for the apoptotic cell density N_2, by using the relation $N_2 = 1 - N_1$. Thus, finally the system (4) becomes

$$\begin{cases} \frac{\partial N}{\partial t} - \nabla \cdot (\nabla p N) = \nabla \cdot (D \nabla N) + \alpha N - \beta N & \text{in} \quad \Omega_c \times (0,T), \\ -\Delta p = \nabla \cdot (D \nabla N) + \alpha N & \text{in} \quad \Omega_c \times (0,T). \end{cases} \tag{5}$$

We remark this is a coupled model, involving a parabolic-type equation for N, the proliferative cell density, and an elliptic-type equation for the pressure p, where p depends implicity on the time variable t, through N. This model will be complete by giving initial (time) boundary conditions for N, boundary conditions for both unknowns N and p, and by assigning values to the parameters D, α and β.

The choice for these boundary conditions and parameters relies on the descriptions that have been reported in the literature (see for instance [19, 42, 43]). We consider two cases. In the first case, that we hereafter call the "normal case" the goal is to have the shape of the crypt Ω_c preserved and a normal distribution of cells along the crypt wall, as recurrently described in the literature. In the second case, hereafter called the "abnormal case", the aim is to recover aberrant colonic crypt shapes (this is also the primary goal of the paper), by using the coupled model (5) and with the presupposition (also often reported in the literature and medically validated experimentally), that an abnormal behavior of the cell dynamics will induce a modification in the shape of the colonic crypt.

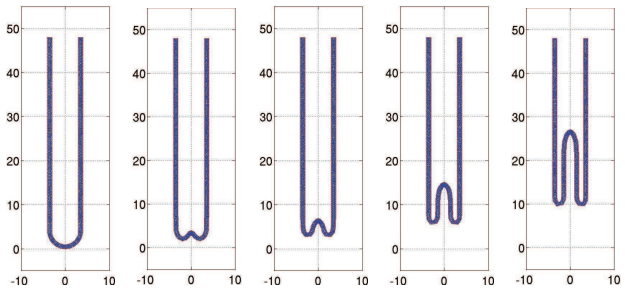

(a) (b) (c) (d) (e)

FIGURE 3. Shape of the colonic crypt for different times: (a) $t = 0$, (b) $t = 1$, (c) $t = 2$, (d) $t = 5$, (e) $t = 10$.

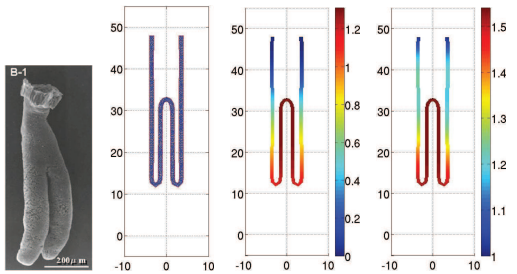

(a) (b) (c) (d)

FIGURE 4. Comparison of a medical image with the numerical simulations (obtained with model (17)-(18)-(19) at final time $T = 40$). (a) Medical image exhibiting a bifurcated colonic crypt (from [21], with permission of Springer). (b) Finite element mesh. (c) Proliferative cell density N. (d) Pressure p.

(sub-figure 4 (a)). The sub-figures (c) and (d) show the proliferative cell density and the pressure, respectively.

5. Conclusions and outlook

The main purpose of this paper has been to simulate colonic crypt bifurcation, by means of partial differential equations, more exactly, by using a convection-diffusion-shape model. This model couples the dynamics of live

Algorithm - abnormal case.

Step 1 Initialize at time $t = 0$, with $\Omega_c 0 = \Omega_c$, $\Gamma_1 0 = \Gamma_1$, $\Gamma_2 0 = \Gamma_2$, $\Gamma_3 0 = \Gamma_3$, $N0$ defined in (6), and p^{*0} the solution of (20). Determine the pressure $p0$ by solving (20).

Step 2 For $i \geq 0$:

(a) Determine N^{i+1}, the solution of (17) in the current domain Ω_c^i, using the previous computed p^i.

(b) Define the new domain Ω_c^{i+1}, by determining the new boundaries Γ_3^{i+1}, Γ_2^{i+1} as indicated in (22)–(23), and with $\Gamma_1^{i+1} = \Gamma_1$, for all $n \geq 1$.

(c) Define a new finite element mesh in the new domain Ω_c^{n+1}.

(d) Define the extension N^{i+1} to the new domain Ω_c^{i+1}, such that

$$N^{i+1}(x^{i+1}, y^{i+1}) = N^i(x^i, y^i)$$

where the points $(x^{i+1}, y^{i+1}) \in \Omega_c^{i+1}$ and $(x^i, y^i) \in \Omega_c^i$ either coincide, or are related by (22) or (23).

(e) With N^{i+1} determine p^{*i+1} and afterwards p^{i+1} in the new domain Ω_c^{i+1} (using (20) and (18), respectively).

Step 3 Go to Step 2 and repeat with i replaced by $i + 1$.

Step 4 Stop when the final time T is reached.

4.2.1. *Experiments - abnormal case.* Here we use the same values described before, in section 3.2.1, for the rectangle, Ω, the crypt domain at time $t = 0$, *i.e.* $\Omega_c(0) = \Omega_c$, and the parameters ϵ, τ_1, and τ_2. The new parameter γ is equal to 10. Again, the spatial domains Ω and Ω_c are discretized with triangular finite element meshes and linear shape functions. The implementation is done in MATLAB® [40].

For each domain $\Omega_c(t)$ the time step size verifies $dt < \frac{c}{b}\min(dx, dy)$, where c is a constant less than 1, b is the maximum of the normal velocity v_n euclidean norm, in $\Gamma_3(t)$, *i.e.* $b = max|v_{n|\Gamma_3(t)}|$, and dx and dy are the spatial step sizes in the OX and OY directions, respectively.

In Figure 3 we can see the beginning and the evolution of the bifurcation process in a colonic crypt. By increasing the proliferative rate, at the bottom of the crypt, the pressure becomes larger there, and leads to a deformation of the outer and inner boundaries $\Gamma_2(t)$ and $\Gamma_3(t)$.

The Figure 4 displays the shape of the crypt at final time $T = 40$, and illustrates the similarity with the bifurcation observed in a medical image

3. Normal Case

Boundary conditions for N. The initial (time) condition for the proliferative cell density we set $N(0, x, y) := N^0(x, y)$, where

$$N0(x, y) := \frac{1}{2}(1 + \frac{2}{\pi}\arctan(\frac{\frac{2h}{3} - y}{\epsilon})) \tag{6}$$

where h is the height of the crypt (measured along the crypt axis $\overrightarrow{OY}$, see Figure 1 (b), and ϵ is a very small positive scalar (see section 3.2.1, for the exact values of h and ϵ). This definition is in good agreement with experiments and literature (see for instance [8]), where it is claimed, the proliferative cell activity occurs in the lower two-third part of the crypt. In effect N^0 is then approximatively 1 and zero at the bottom and top of the crypt, respectively.

In addition we set

$$\begin{aligned} N(t, x, y) &:= 0 \quad \text{in} \quad \Gamma_1 \times (0, T), \\ \tfrac{\partial N}{\partial n}(t, x, y) &:= 0 \quad \text{in} \quad \big(\Gamma_2 \cup \Gamma_3\big) \times (0, T). \end{aligned} \tag{7}$$

These two boundary conditions are also reasonable, since, it is well known, that inside a crypt, the cell flux (mainly driven by mitotic-activity, *i.e.* cell division) is directed towards the top, to the crypt orifice. Once the cells reach the top of the crypt they undergo apoptosis. The first condition in (7) simply states that at the top of the crypt there are not proliferative cells and it allows for the shedding of cells into the lumen. The second condition imposes that there is no flux of cells across the lateral boundaries Γ_2 and Γ_3, which is also verified in normal crypts.

Boundary conditions for p (pressure). We set

$$\begin{aligned} p(t, x, y) &:= 1 \quad \text{in} \quad \Gamma_1 \times (0, T), \\ \tfrac{\partial p}{\partial n}(t, x, y) &:= 0 \quad \text{in} \quad \big(\Gamma_2 \cup \Gamma_3\big) \times (0, T). \end{aligned} \tag{8}$$

The first condition (Dirichlet condition) simply states that the pressure is always constant at the crypt orifice, where the apoptotic cells are shed into the lumen. The second condition states that, in normal crypts, the cell flux is directed upwards and not laterally. This means that the normal velocity of the cells on Γ_2 and Γ_3 verifies $v \cdot n = 0$, where n is the unit outward normal vector to the boundary of Ω_c. Thus, and because of (3) (which states $v = -\nabla p$), we have $0 = \frac{\partial p}{\partial n}$ in Γ_2 and Γ_3.

Choice of the parameters D, α and β. We emphasize that the values for these parameters are not known. However there is some qualitative informative about them, that we use in the sequel for their definition.

As mentioned before, the proliferative cells are essentially located in the lower two-thirds of the crypt, with a strong activity at the bottom of the crypt, while the fully differentiated and apoptotic cells are located in the upper third part of the crypt. Accordingly, we choose for α a decreasing function of the height of the crypt (quadratic at the crypt bottom), that must be zero in the upper third top part (see also [45], where the rate of birth α is a linear function of the crypt height). For defining β, the rate of death of the proliferative cell density N, we just adopt the reverse definition of α. Thus,

$$\alpha(y) := \begin{cases} (y-\frac{2}{3}h)2\,\tau_1 & y \in [0,\frac{2}{3}h] \\ 0 & y \in [\frac{2}{3}h,h] \end{cases}, \qquad \beta(y) := \begin{cases} 0 & y \in [0,\frac{2}{3}h] \\ (y-\frac{2}{3}h)2\,\tau_2 & y \in [\frac{2}{3}h,h] \end{cases} \tag{9}$$

where τ_1 and τ_2 are two positive small weighting parameters (see section 3.2.1, for their values).

The diffusion coefficient D is usually considered a constant. So we hereafter set $D := 1$. Other definitions might be also possible, as for instance, a function of the height of the crypt, like α and β, or a function of the unknown cell density N (see [4, 35]).

3.1. Mathematical model - normal case. By gathering all these previous definitions and equations, we can now formulate the mathematical model for the normal cell dynamics inside the colonic crypt. Find N (the proliferative cell density) and p (the pressure related to the convective velocity v, by the equation $v = -\nabla p$), such that

$$\begin{cases} \frac{\partial N}{\partial t} - \nabla\cdot(\nabla p N) = \nabla\cdot(D\nabla N) + (\alpha-\beta)N & \text{in} \quad \Omega_c\times(0,T), \\ -\Delta p = \nabla\cdot(D\nabla N) + \alpha N & \text{in} \quad \Omega_c\times(0,T), \\ p = 1 & \text{in} \quad \Gamma_1\times(0,T), \\ \frac{\partial p}{\partial n} = 0 & \text{in} \quad \big(\Gamma_2\cup\Gamma_3\big)\times(0,T), \\ N = 0 & \text{in} \quad \Gamma_1\times(0,T), \\ \frac{\partial N}{\partial n} = 0 & \text{in} \quad \big(\Gamma_2\cup\Gamma_3\big)\times(0,T), \\ N(0,.) = N0(.) & \text{in} \quad \Omega_c, \end{cases} \tag{10}$$

with $D = 1$, α, β defined in (9), and N^0 in (6).

The problem (10) is a coupled problem. In order to solve it we basically decouple N and p. We first solve the elliptic-tye equation for p, with a given N, and afterwards the parabolic-type equation for N, with the previous computed p, and this procedure is iterated on time. This methodology is explained in the next section (see algorithm (3.2)). In the appendix we

and the rate of birth α is now defined, with a higher value at the bottom of the crypt (compare with (9))

$$\alpha(x,y) := \begin{cases} (y-\frac{2h}{3})2\tau_1 + \dfrac{1}{\sqrt{x2+\frac{(y-0.5)2}{900}}+1} & y\in[0,\frac{2}{3}h],\ |x|<0.5, \\ (y-\frac{2h}{3})2\tau_1 & y\in[0,\frac{2}{3}h],\ |x|\geq 0.5, \\ 0 & y\in[\frac{2}{3}h,h]. \end{cases} \tag{21}$$

Moreover, we assume, that for each time t, the boundary condition for the pressure in the inner lateral boundary $\Gamma_3(t)$ of the crypt should be proportional to the difference between the current pressure $p(t)$ and the normal pressure p^*. That is, $\frac{\partial p(t)}{\partial n} = -\gamma(p(t)-p^*)$, where γ is a positive scalar (its value is defined in section 4.2.1). Therefore, since the velocity of the proliferative cell density N verifies (3), the normal velocity at each point of this inner lateral boundary is $v_n(t) = \gamma\big(p(t)-p^*\big)$. In particular, it points outwards the crypt if $p(t) > p^*$. Thus, motivated by this latter property, we redefine the shape of the inner lateral boundary, at time $t+dt$, where dt is a very small positive time increment, by using the following first-order Taylor formula: any point $(x,y)(t+dt)$ belonging to $\Gamma_3(t+dt)$ is derived from the corresponding point $(x,y)(t)$ in $\Gamma_3(t)$, by

$$(x,y)(t+dt) := (x,y)(t) + dt\, v_n(t)\, n(t), \tag{22}$$

where $v_n(t)$ is the the normal velocity at point $(x,y)(t)$ (given by $v_n(t) = \gamma\big(p(t)-p^*\big)$), and $n(t)$ is the unit outward normal vector to the boundary $\Gamma_3(t)$, at the point $(x,y)(t)$. In addition, since in a normal 2D-crypt, the inner region is a thin layer, whose thickness corresponds to the size of only one cell, we assume the deformation undergone by $\Gamma_2(t)$ follows $\Gamma_3(t)$. This means, we suppose that a single cell deforms like an entire body. Consequently, any point $p_{\Gamma_2(t)}$ of $\Gamma_2(t)$, lying on the straight-line defined by the unit outward normal vector to a point $p_{\Gamma_3(t)}$ of $\Gamma_3(t)$, verifies

$$v_n(p_{\Gamma_2(t)}) := -v_n(p_{\Gamma_3(t)}). \tag{23}$$

In this way, the thickness of the region inside the crypt domain, $\Omega_c(t)$, is always the same and fixed, for any time t.

4.2. Numerical approximation - abnormal case. Likewise the normal case we use finite elements for discretizing the space variable (x,y) and finite differences for the variable t. The procedure for solving the abnormal case is summarized in the following algorithm.

should change the velocity v (3) of the flux of cells, as well as the pressure p on the lateral boundaries Γ_2 and Γ_3. On the whole this would promote a change in the geometry of the colonic crypt.

4.1. Mathematical model - abnormal case. The mathematical model for the abnormal case has a structure somewhat similar to (10), with respect to the cell dynamics. The main difference is that it is now formulated in a time dependent crypt domain with moving boundaries. It is composed of three parts: the coupled parabolic and elliptic equations, involving the unknowns N and p, and the equation describing the evolution the spatial domain Ω_c.

Abnormal cell dynamics - N equations

$$\begin{cases} \frac{\partial N}{\partial t} - \nabla \cdot (\nabla p N) = \nabla \cdot (D \nabla N) + \alpha N - \beta N & \text{in} \quad \Omega_c(t) \times (0,T), \\ N = 0 & \text{in} \quad \Gamma_1(t) \times (0,T), \\ \frac{\partial N}{\partial n} = 0 & \text{in} \quad \big(\Gamma_2(t) \cup \Gamma_3(t)\big) \times (0,T), \\ N(0,.) = N0(.) & \text{in} \quad \Omega_c(0) = \Omega_c. \end{cases} \tag{17}$$

Abnormal cell dynamics - p equations

$$\begin{cases} -\Delta p = \nabla \cdot (D \nabla N) + \alpha N & \text{in} \quad \Omega_c(t) \times (0,T), \\ p = 1 & \text{in} \quad \Gamma_1(t) \times (0,T), \\ \frac{\partial p}{\partial n} = 0 & \text{in} \quad \Gamma_2(t) \times (0,T), \\ \frac{\partial p}{\partial n} = -\gamma(p - p^*) & \text{in} \quad \Gamma_3(t) \times (0,T). \end{cases} \tag{18}$$

Time dependent crypt domain and moving boundaries

$$\begin{cases} \Omega_c(0) := \Omega_c, \\ \Omega_c(t) := \text{crypt domain at time } t \in (0,T], \quad \partial\Omega_c(t) := \Gamma_1(t) \cup \Gamma_2(t) \cup \Gamma_3(t), \\ \Gamma_1(t) := \Gamma_1, \forall t \in [0,T], \quad \Gamma_2(t) \text{ and } \Gamma_3(t) \text{ are defined in (23) and (22).} \end{cases} \tag{19}$$

Here $D = 1$, β is defined in (9), $N0$ in (6); p^* is the normal pressure obtained by solving the elliptic equation in (10), in the time dependent domain $\Omega_c(t)$, *i.e.*

$$\begin{cases} -\Delta p = \nabla \cdot (D \nabla N) + \alpha N & \text{in} \quad \Omega_c(t) \times (0,T), \\ \frac{\partial p}{\partial n} = 0 & \text{in} \quad \big(\Gamma_2(t) \cup \Gamma_3(t)\big) \times (0,T), \\ p = 1 & \text{in} \quad \Gamma_1(t) \times (0,T), \end{cases} \tag{20}$$

also comment on the existence and regularity of the solutions to these two decoupled problems.

3.2. Numerical approximation - normal case. In order to actually compute the finite-dimensional approximation to the solution of (10), we need to define the discretization employed. We applied finite elements, for discretizing the space variable (x, y), and finite differences for the time variable t. Thus, by first applying the finite element method, we have the following semidiscrete Galerkin formulation (discrete in space and continuous on time), of (10)

$$\begin{cases} M \frac{\partial N}{\partial t}(t) + C(p)N(t) = -KN(t) + M_{(\alpha-\beta)}N(t), & \text{in } (0,T) \\ Kp = -KN(t) + M_\alpha N(t), & \text{in } (0,T) \\ N(0) = N0. \end{cases} \tag{11}$$

Here, M and K are the usual mass and stiffness finite element matrices, M_α and $M_{(\alpha-\beta)}$ are modified mass matrices (resulting directly from the generation of matrices by the finite element procedure) and $C(p)$ is also a finite element matrice, depending on the pressure p, that comes from the pressure equation. We denote by p and $N(t)$ the finite element approximations of $p(.)$ and $N(t,.)$, respectively. This means that now p and $N(t)$ are vectors of unknowns at the finite element nodes. In addition N^0 is also the finite element vector corresponding to the function defined in (6). We represent by $\frac{\partial N}{\partial t}(t)$ the derivative of the vector $N(t)$ with respect to the time variable. Let us now proceed and subdivide the time interval $[0,T]$ into $n-1$ subintervals

$$[0,T] = \bigcup_{i=0}^{n-1} [t_i, t_{i+1}], \qquad 0 = t_1 < t_2 < \ldots < t_i < \ldots < t_n = T$$

We assume, for simplicity, the time step size $dt = t_i - t_{i-1} = \frac{T}{n-1}$ is constant over the time interval. In addition, we approximate the time derivatives $\frac{\partial N}{\partial t}(t_{i+1})$ by the forward time difference scheme

$$\frac{\partial N}{\partial t}(t_{i+1}) \approx \frac{N(t_{i+1}) - N(t_i)}{dt} = \frac{N^{i+1} - N^i}{dt} \tag{12}$$

where the notations are self-explanatory. Consequently, we fully discretize the equations (11), by the following system of equations

$$\begin{cases} M \frac{N^{i+1} - N^i}{dt} + C(p)N^{i+1} = -KN^{i+1} + M_{(\alpha-\beta)}N^{i+1}, \\ Kp = -KN^i + M_\alpha N^i, \end{cases} \tag{13}$$

for all $i = 0, \ldots, n-1$. This scheme corresponds to implicit (or backward) Euler time discretization method, for the equation with unknown N. The

coupled system (13) can equivalently be rewritten as

$$\begin{cases} \left(\frac{M}{dt} + C(p) + K - M_{(\alpha-\beta)}\right) N^{i+1} = \frac{M}{dt} N^i, \\ Kp = (-K + M_\alpha) Ni, \end{cases} \tag{14}$$

for all $i = 0, \ldots, n-1$.

The methodology we apply to solving the discrete problem (14) is next described.

Algorithm - normal case.

Step 1 Initialize at time $t = 0$, with $N0$ given by (6) and $p0$ the solution of

$$Kp = (-K + M_\alpha) N^0.$$

Step 2 For $i \geq 0$:

(a) Determine N^{i+1}, with the previous p^i, by solving

$$\left(\frac{M}{dt} + C(p^i) + K - M_{(\alpha-\beta)}\right) N^{i+1} = \frac{M}{dt} N^i.$$

(b) Determine p^{i+1}, the solution of $Kp^{i+1} = (-K + M_\alpha) N^{i+1}$.

Step 3 Go to Step 2 and repeat with i replaced by $i + 1$.

Step 4 Stop when the final time T is reached.

3.2.1. *Experiments - normal case.* For all the experiments we take dimensionless values, and the following have been used, unless otherwise mentioned. The final time is $T = 10$. The size of the 2D crypt $\Omega_c \subset \mathbb{R}2$ (see sub-figure 1 (b)) is based on average dimensions reported on the literature for human colonic crypts, as described before in section 2. We consider the rectangle $\Omega = [-10, 10] \times [-5, 55]$ and for the boundary of Ω_c (see again sub-figure 1 (b)), denoted by $\partial\Omega_c = \Gamma_1 \cup \Gamma_2 \cup \Gamma_3$,

$$\begin{aligned} \Gamma_1 &:= \{(x, y) \in \mathbb{R}2 : (-4 \leq x \leq -3 \vee 3 \leq x \leq 4) \wedge y = 48\}, \\ \Gamma_2 &:= \{(x, y) \in \mathbb{R}2 : (x = -4 \vee x = 4) \wedge 4 < y < 48\} \cup \{(x, y) \in \mathbb{R}2 : y = 4 - \sqrt{16 - x2}\}, \\ \Gamma_3 &:= \{(x, y) \in \mathbb{R}2 : (x = -3 \vee x = 3) \wedge 4 < y < 48\} \cup \{(x, y) \in \mathbb{R}2 : y = 4 - \sqrt{9 - x2}\}. \end{aligned} \tag{15}$$

The parameters ϵ, τ_1, τ_2 and h, in the definition of $N0$, α and β (see (6) and (9)), are equal to 4.8, 10^{-5} , 10^{-3} and 48, respectively.

The spatial domains Ω and Ω_c are discretized with triangular finite element meshes and linear shape functions. The implementation is done in MATLAB® [40].

The Figure 2 displays the result of the numerical simulations for final time $T = 10$. In particular, the sub-figure (b) shows that the function N respects

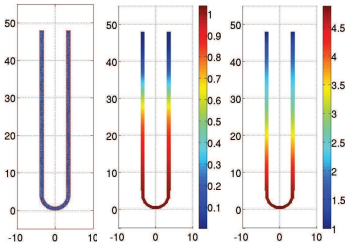

FIGURE 2. Normal crypt simulations for final time $T = 10$. (a) Finite element mesh. (b) Proliferative cell density N. (c) Pressure p.

the distribution of proliferative cells, along the crypt height, in a normal colonic crypt.

We observe that we assigned values to the parameters ϵ and τ_2, but the choice 10^{-5}, related to the rate of proliferation, was made differently. We executed the algorithm 3.2, for a finite set S of τ_1 values, and computed the value τ_1^* leading to

$$\min_{\tau_1 \in S} \|N^{n_{max}} - N^0\|, \tag{16}$$

where n_{max} is the last iteration in algorithm 3.2, corresponding to the final time T. The result was $\tau_1^* = 10^{-5}$, and consequently in (9), $\tau_1 = \tau_1^* = 10^{-5}$. The corresponding pressure, denoted hereafter by p^*, will be used in the abnormal case problem: this p^* will be henceforth considered the "normal pressure" in a normal colonic crypt.

4. Abnormal case

The primary goal of this paper is to recover aberrant crypt shapes, by using the dynamics of proliferative cells inside the crypt. In the previous "normal case", the focus was on the cell dynamics, yielding a stabilized crypt shape. As opposed to this "normal case", now we perturb this normal cell mechanism, inside the crypt, check whether it disrupts the U-shape geometry of the normal crypt, and recover abnormal crypt shapes (as in [21, 38]). It is in effect widely reported in the literature, and also validated experimentally, that an abnormal shape of the colonic crypt could be associated to a modification of the rate of birth α, of the proliferative cell density N. An increase of α